Research Square

Preprints are preliminary reports that have not undergone peer review.
They should not be considered conclusive, used to inform clinical practice,
or referenced by the media as validated information.

Granular Mesoporous Carbon Using Soft Template as a Support for Synthesis of HDS Catalyst

maryam soleymani
Tarbiat Modares University (TMU)
Ramin Karimzadeh
ramin@modares.ac.ir

Tarbiat Modares University (TMU)
Alimorad Rashidi
Research Institute of Petroleum Industry (RIPI)
ali eslamimanesh
Tarbiat Modares University (TMU)

Research Article

Keywords: Mesoporous activated carbon, Soft template, Catalyst support, HDS

Posted Date: March 7th, 2024

DOI: https://doi.org/10.21203/rs.3.rs-3994782/v1

License: This work is licensed under a Creative Commons Attribution 4.0 International License.
Read Full License

Additional Declarations: No competing interests reported.

Abstract

Background

This research aims to synthesize a novel granular mesoporous activated carbon (AC). The produced carbon is utilized as a support for synthesis of a catalyst of hydrodesulfurization (HDS) process of a heavy naphtha sample. The novel AC benefits from a high mechanical strength despite its mesoporous structure originating from removing the existing defects.

Methods

A combination of binders with soft template is applied on the carbon to enhance its mechanical strength and establish its mesoporous structure. Also, effects of acid modification to the binder on the mechanical properties and surface characteristics of AC are investigated. Also, a Fe-Mo catalyst is synthesized on the prepared and commercial AC, and is tested for HDS process.

Significant findings

Accordingly, the results show that the average pore size and specific surface area of AC are increased significantly. Also, results showed that use of a combination of the cellulosic binder and the organic acid leads to the creation of a mesoporous structure in carbon with an average pore size of 5.6 nm, while inorganic acid creates micropore structure. The results indicate that sulfur conversion of feed at atmospheric pressure, using the prepared catalyst, is 80% while the synthetic catalyst on commercial AC-support brings 66% conversion.

1. Introduction

Activated carbon, whether in powdered or granular form, has wide applications in industry. It can be used as an adsorbent, catalyst support, or electrode.[1–4] Among the properties of activated carbon which make it suitable for specific applications, the size of pores in its structure including micropores, mesopores, and macropores is of particular importance. In this regard, the mesoporous structure benefits from its superior affinity for adsorbing large molecules compared to the others. In addition, the mesopores are not blocked when large molecules are passed through in adsorption process.[5–9] The latter structure, when used to synthesize a catalyst support, prevents the blocking of materials during metal impregnation and consequently improves the performance of the catalyst compared to e.g. a catalyst made on a microporous structure support.[10–15]

In recent years, substantial research has been done in order to improve the performance of catalysts produced on carbon supports. The main reason is that unlike the conventional metal oxide catalyst bases, carbon supports have a low tendency for coke deposition[16–19] due to their high capacity of hydrogen adsorption on their surface.[20] On the other hand, the mentioned catalysts have shown superior performance in processes such as hydrodesulfurization (HDS) of petroleum cuts.[13, 21, 22] Weaker

interaction between the carbon support material and the active metal (and consequently more active sites on their surface) as well as relatively high specific surface area are perhaps the most important factors for the latter finding.[13, 21, 22]

Various studies related to desulfurization processes have shown that the size of sulfur-containing molecules and the size of holes present in the structure of catalysts supports have direct impacts on the efficiency of the utilized catalysts.[23] For instance, a catalyst made on mesoporous alumina was demonstrated to have significant ability for removing dibenzothiophene (DBT) and thiophene from various hydrocarbon feeds.[24] Furthermore, a comparison between different supports including alumina, silica, and carbon for removal of sulfur-bearing compounds with large molecules showed that supports with mesoporous structures lead to higher percentage of removals.[11] Farag and coworkers [26] have noted that their studied Co-Mo/carbon catalysts exhibit higher HDS efficiency for removal of dibenzothiophene from diesel fuel than desulfurization percentage achieved using a commercial Co-Mo/Al_2O_3 catalyst.[16, 25]

In another research, the influence of pore size of a catalyst base on its performance for sulfur removal from aromatic rings present in a petroleum fluid was investigated. It was shown that catalysts with large pores in their support structures (with 14 nm average diameter) exhibit higher efficiency compared to the catalyst made on a support with smaller pores (with 7 nm average diameter).[10] Other works[12–14] have concluded that depending on the molecular sizes of the sulfur compounds, performance of catalysts for their removal is significantly different. Accordingly, smaller sulfur-bearing compounds such as thiophene and DBT can be removed with higher yields using the catalysts made on carbon bases while catalysts produced on alumina support are reported to be more suitable for removal of sulfur compounds with larger molecules.[12–14] Moreover, Guojun et al.[26] have synthesized Co-Mo and Ni-Mo catalysts on the mesoporous carbon support, a commercial active carbon, as well as alumina. Their produced mesoporous carbon was shown to have specific surface areas of 1400 to 2000 m^2/g and the diameters of the pores of 2 to 3 nm. They also found that Co-Mo/mesoporous carbon catalyst is significantly more active than Co-Mo/γ-Al_2O_3 and Co-Mo /activated carbon catalysts for hydrodesulfurization of thiophene from gasoline model fuel.

Various methods have been used to control pore size of carbon. In a research, CMC mesoporous carbon was produced from fructose and wheat flour precursors, and $ZnCl_2$ was used in different proportions to control pore size of carbon. They used the produced mesoporous carbon as a catalyst base for the HDS process. Their results showed that Co-Mo/mesoporous carbon was significantly more active than both Co-Mo/γ-Al_2O_3 and Co-Mo. / Activated carbon for hydrodesulfurization of thiophene from gasoline model fuel. [26, 27] In another research, the activated carbon prepared from rubber waste was modified with two sources of HNO_3 and NaOH, as a result of which the activated carbon modified with HNO_3 could absorb larger sulfur molecules due to its larger pores.[28, 29]

However, although the above advantages of activated carbon supports have made them to become an interesting candidate to be used for synthesis of HDS catalysts, they are still not industrially-commercialized due to their low mechanical strength, small pore diameters, low acidity, considerable number of blocked pores after granulation, and their non-negligible weight loss during long continuous high temperature processes. In this work, a mesoporous granular activated carbon with high mechanical strength was synthesized from a grapevine branch and oil palm trunk sources. In addition, a material comprising a combination of binders was used to enhance the mechanical strength of the granular carbon while maintaining its mesoporous structure as well as its stability in water.

2. Materials and methods

2.1. Materials

Nitric acid 68%, phosphoric acid 85%, citric acid 99%, and carboxy methyl cellulose (CMC) were supplied by Merck. Coal tar pitches were procured from Isfahan Coal Tar Refinery, Isfahan, Iran. Grape branch and oil palm trunk were collected from orchards located in two Iranian cities of Tehran, and Shiraz, respectively. Ammonium heptamolybdate and iron (III) nitrate with 99% purity were purchased from Merck.

2.2. Synthesis of mesoporous granular activated carbon

In the present study, 5 activated carbon samples were synthesized. For all the produced samples, activated carbon powder was synthesized from a mixture of a portion of the grape branch and the palm trunk. [30] Briefly, the mentioned source material were ground and were sieved. Then, the obtained material was dried at 120°C for 24 h followed by mixing with a mixture of phosphoric acid (85, wt%) and nitric acid (68, wt%) at room temperature. The impregnation ratio of mixed acid to precursor is 4 wt/wt. The sample was then dried in the oven at 110°C for 48 h. In the next step the dried materials was carbonized under nitrogen flow of 100 ml/min with temperatures raised in one steps with the rate of 8°C/min to 600°C. Sample were kept at 600°C for 1.5h. Finally, the obtained activated carbon was washed with boiling distilled water until reaching neutral pH and was dried in an oven for 24 h.

Except for sample G1 (see Table 1) which was produced in a powder form, granulation of the produced activated carbon samples took place in the following steps: Addition of a binder made from mixing the cellulosic binder (CMC) with coal tar pitch for sample G2; modification of the binder was made with phosphoric acid for sample G3 and with citric acid for samples G4 and G5. In the next step, all samples were extruded using an extruder with 2 mm diameter and 6 mm length. After extrusion, obtained samples were dried at ambient temperature for 24 h. Then, the materials was carbonized under nitrogen flow of 100 ml/min with temperatures raised in three steps with the rate of 2°C/min to 300°C, with 3°C/min rate to 600°C and with rate of 8°C/min up to 830°C. Samples were kept at each temperature for 40 min. Finally, the samples were cooled in the nitrogen atmosphere. The materials utilized for granulation of each activated carbon sample are reported in Table 1.

Table 1
Operating conditions for granulation of activated carbon samples.

Sample	Binder	Binder modification	Step of modification
G1	None	None	None
G2	CMC + coal tar pitch	None	None
G3	CMC + coal tar pitch	H_3PO_4	before carbonization
G4	CMC + coal tar pitch	citric acid, 50 wt%	before carbonization
G5	CMC + coal tar pitch	citric acid, 30 wt%	before carbonization

2.3. Fe-Mo loading

The wet impregnation method was used to prepare the catalysts. The metals were loaded on the support with the weight ratio of Mo:Fe equal to 3. For the preparation of the catalysts, 5 g of each activated carbon samples were added to an aqueous solution containing 1.1 g ammonium heptamolybdate, 1.2 g iron nitrate, and an appropriate amount of citric acid. The mixture was stirred at 50°C until the sample became a paste, then it was dried in an oven at a temperature of 90°C for 24 h. After that, the samples were heated to 450°C with 5°C/min, and calcined at 450°C for 3h under nitrogen atmosphere with 50 ml/min. As will be discussed later in the article, two catalysts samples were synthesized using activated carbon supports of G4 and G6 (commercial activated carbon) with the properties reported in Table 3 designated as FeMo-G4 and FeMo-G6, respectively.

2.4. Characterization analyses

Different analytical tests were conducted on the prepared samples in order to determine their characteristics. The Brunauer-Emmett-Teller (BET) and Barrett-Joyner- Halenda (BJH) techniques were used to obtain the specific surface area of granular activated carbons and their pore sizes, respectively. In order to obtain the specific surface area, the samples were first degassed at 200°C for 2h. Then, the adsorption isotherm was obtained at 77 K under nitrogen atmosphere using A Micromeritics Porosimeter ASAP 2010. Crush strength analysis was performed for evaluation of the mechanical strength of the granules. This test method includes determining the resistance of formed catalysts and catalyst carriers against compressive force and can be used for regular catalyst shapes. This test method determines the average crush strength in the range from 0 to 220 N. The TGA analysis was conducted for determination of their temperature stability. Moreover, surface morphologies of the prepared activated carbons as well as the synthesized catalysts were studied through FESEM analysis. Additionally, XRD (Siemens, model D5000) test was used to identify the phases present in the activated carbons and catalysts structures. The functional groups formed on the surface of the produced samples were also determined by FTIR spectrum analysis (Bruker, Alpha Series spectrophotometer). The transmission FTIR spectra of samples were obtained with a Nicolet 20 SXB spectrophotometer using pellets of KBr containing about 0.5% sample. The samples are dried at 100 degrees Celsius for 24 hours before analysis

2.5. Catalytic activity tests

A fixed-bed HDS reactor made of stainless steel with an internal diameter of 1 cm was employed to measure the activity of the prepared catalysts. Details of the experimental set-up can be found elsewhere.[31] Temperature is measured through three temperature probes (with an uncertainty of 2 ^{o}C). Through a HDS process at atmospheric pressure, sulfur-bearing species were removed from a heavy naphtha sample with around 900 ppm total sulfur (the characteristics of heavy naphtha are given in the Table 2). For this purpose, the stream containing the petroleum fluid and N_2 and H_2 was fed to the reactor. After desulfurization reactions took place, the product was separated from the gas phase utilizing two separators followed by H_2S removal by a caustic wash.[32] In order to prepare the catalysts to be used in the described process, 2 g of each catalyst was mixed with carborundum with a weight ratio of 1:2, then was sulphided with $H_2 + H_2S$ feed with a weight ratio of 10:1 and a flow rate of 100 ml/min. The catalyst was sulfided with temperatures raised in two steps with the rate of 15°C/min to 100°C, with 8°C/min rate to 400°C. Samples were kept at 400°C for 2h. Other operational parameters reaction step are as follows: liquid hourly space velocity (LHSV) = 4, H_2/feed volume ratio = 180 Nlit/lit, T = 280 and 340°C, and P = 1 atm. The final HDS process product was sampled from the separator tank and was analyzed to measure its total sulfur.

Table 2
property of reaction feed

Property	Density at 15.56°C	IBP (°C)	Total Sulfur %
Naphtha	0.70	92	0.09

3. Results and discussion

3.1. Impacts of binder

As pointed out earlier, suitable mechanical strength is essential for an activated carbon support to be used for producing industrial catalysts. It has been suggested that addition of particular binders can increase the mechanical strength of carbon though it might decrease its specific surface area (S_{BET}) as well as its average pore size at the same time.[33]

In the present study, two types of materials were used to make a combined binder in order to fulfill the above requirements. The first binder material is a CMC, which causes initial shaping of the activated carbons. In other words, CMC creates a binder paste for the material to be able to be extruded. However, since the CMC bonds with carbon are either weakened or broken above 300 ^{o}C, the resulted material would not be stable in water after a water wash. In order to enhance the corresponding stability, another binder-type material needs to be used.[34–36] Subsequently, coal tar pitch was added to the CMC binder which brings about high waterproofing property and can simultaneously enhance the mechanical

strength of the activated carbon samples.[37–41] Despite the appropriate properties that the latter combination offers, the added coal tar pitch can diffuse into the carbon mesopores creating Carbon-Carbon bonds at high temperatures which can eventually alters the carbon structure to become microporous.[42–44]

Previous studies[42–44] have shown that even with addition of materials such as coal tar pitch to the basic binder, the carbon structure is still not completely mesoporous. In order to overcome the mentioned obstacle, the combined binder materials were either modified with phosphoric or citric acid (see Table 1). For making the final binder, appropriate proportions of CMC and coal tar pitch were mixed. The mixed percentages of the two latter substances were kept constant in all experiments. Later, two weight percentages of citric acid were added to the previous mixture according to Table 1. The obtained samples were tested to determine the required properties which are reported in Table 3. BJH pore size distribution graphs of granular activated carbons are shown in Fig. 1.

Table 3
Properties of the synthesized granular activated carbon samples along with a commercial material.

Sample NO.	Quality of appearance of the bodies	Stability in water	BET area (m^2/g)	Total pore volume (cm^3/g)	Volume of micropores (cm^3/g)	Average pore size (nm)	Crush strength N/cm
G1	-	-	1610	1.75	0.29	4.47	-
G2	Good	Good	650	0.46	0.05	2.81	400
G3	Poor	Poor	-	-	-	-	-
G4	Good	Good	950	1.16	0.09	5.60	276
G5	Good	Good	1240	1.30	0.12	4.30	290
G6*	Good	Good	1463	0.93	0.40	2.54	500

*Commercial activated carbon material.

The binder used in synthesis of sample G2 (see Table 1) is a combination of CMC and coal tar pitch which creates relatively high mechanical strength (around 400 N/cm); however, the specific surface area of the sample was reduced from 1610 m^2/g to 650 m^2/g after granulation. In addition, its average pore size was reduced from 4.47 nm in powder form to 2.81 nm in granular form. The mentioned finding is consistent with the results reported in the literature demonstrating that coal tar pitch causes the formation of micropores in the carbon structure.[45, 46] As a result, sample G2 is not suitable to be used as the HDS catalyst support.

As reported in Table 3, the obtained results indicate that sample G3 suffer from poor stability in water that can be mainly due to the presence of phosphate remaining in the granule after calcination. As a consequence, the performed water wash can dissolve phosphate which disintegrates the granular structure .[47] A comparison between samples G2 and G4 shows that the applied organic acid reduces the crush strength from 400 N/cm for the former to 276 N/cm for the latter sample along with acceptable stability of the sample in water though the average pore size increases from 2.81 nm for sample G2 to 5.6 nm for sample G4. The current crush strength value is an acceptable value for the catalyst base of the HDS process.[48] The main reason for creation of mesopores in the granular structure of G4 is the molecular structure of the applied binders as follows: Citric acid that was added to produce the binder material links with the CMC and a branched carbon structure is subsequently created. The created branched structures are broken after calcination and mesopores are formed as a result.[49] In addition, the previously formed pores can coalescence together due to the binder addition and create new pores.[50]

It was also found that the mechanical strength of sample G4 is slightly lower than for sample G2 because the former sample has higher pore volume. However, compared to the typical mechanical strength for conventional carbon supports used for producing the commonly-utilized catalysts in industry (around 120 N/cm), sample G4 exhibits acceptable value for this property. Sample G5, on the other hand, was shown to have a higher specific surface area relative to sample G4 due to less amount of organic acid utilized for its synthesis with reduced pore sizes. It should be noted that for comparison purposes, similar tests were conducted on sample G6 which is a commercial granular activated carbon. The conclusion of the analyses described in this section was that due to the advantages of the granular activated carbon (sample G4) including its high specific surface area, suitable mesoporous structure, and acceptable mechanical strength compared to the other synthesized samples as well as a commercial material, it was chosen for further analyses of its properties.

3.2. Characterization of activated carbon samples

The XRD patterns of synthetic activated carbon (sample G4) as well as of the commercial sample are plotted in Fig. 2. It is found that there is a broad peak in the range of 2θ = 26 (002) and 43 (101) degrees can be seen, which indicates the graphite crystallite in structure of the composite.[11] From the XRD pattern, it can be suggested that activated carbons consist of a mixture of amorphous and crystalline structure.[51] Comparing the XRD spectra of two studied samples, it can be seen that diffraction peaks are sharper for the G4 material demonstrating its higher portion of crystallite size in G4 sample.[52] The smaller the value of carbon crystallites leads to the higher the degree of graphitization. So when graphite crystallite scale decreases, which can lead to widening or internal structure disordered, so as to form a larger specific surface area. Therefore, it is expected that the specific surface area of activated carbon G4 is smaller than that of G6. And the irregularity and pores of synthetic activated carbon are more and therefore the average pore size in G4 sample is bigger. [52]

FT-IR spectroscopy technique was used to identify functional groups on the surfaces of samples G4 and G6, as shown in Fig. 3. It is inferred from the plot that bonds in wavelength ranges 3750, 2350, 1530–

1570, and 1060–1200 cm^{-1} are related to functional groups of the synthesized activated carbon. The band in the region 1050–1150 cm^{-1} indicates the C–O–C vibration in cellulose and hemicellulose.[53] In addition, the weak peak in the range of 1100 cm^{-1} corresponds to hydroxyl (C–O).[29, 53–56] A comparison between the commercial activated carbon with the synthetic active carbon shows that the intensity of the peaks in the G4 sample is larger, which indicates the surface oxide functional groups formed on its surface. The presence of the mentioned oxide functional groups generally enhances an increase in the absorption capacity of active metals in the catalyst loading stage. As a result, no further surface modification is needed when sample G4 is used as the catalyst base.[57]

Furthermore, according to Table 4, XRF analysis of samples G4 and G6 reveals that the oxygen content in the former material is higher compared to commercial activated carbon G6. Consequently, it is expected that dispersion of the loaded active metals on the support and ultimately the adsorption efficiency of the synthesized catalyst are augmented for sample G4.[58–60] Apart from that, presence of various phosphorus contents in synthetic activated carbon G4, either before or after acid activation, has a generally positive effect on sulfur removal yield by the final catalyst through a HDS process.[61]

Table 4
Elemental analysis of samples G4 and G6.

Element	Synthetic granular AC (G4)	Commercial AC (G6)
C	75	81
O	18	14
P	5.3	0.4
Others	2.7	0.24

In order to evaluate the surface elemental composition, the chemical as well as electronic states of the elements contained in the synthetic material G4, a XPS test was also performed. Figure 4 illustrates the obtained results from the XPS analysis. As can be seen, the C1s XPS spectrum shows five peaks centered at about 284.5, 285.5, 286, 288.2, and 291.65 eV corresponding to chemical states of carbon as: C – C, C-O, C-O/C-P, C = O, π-π respectively.[47] The carbon-oxygen group in the G4 sample can be either due to the destruction of the carbon structure by the applied acid or can be brought into the activated material from its carbon precursor .[56, 62] Additionally, the peak at 286.5 eV shown in Fig. 4 corresponds to the presence of C-P group revealing that the sample is doped with phosphorus. The determined weight percentages of carbon components from the XPS test are given in the Table 5 which show that about 5 wt% of carbon connections are related to C-P group.

Table 5
Relative amounts of carbon chemical states in G4 sample.

Sample	Chemical groups				
	C-C	C-O	C-P/C-O	C = O	π -π
(G4)	69	12	5	8	6

The FESEM micrographs were taken from sample G1 and G4. As can be seen from the corresponding images shown in Fig. 5, the mesoporous structure of the synthesized activated carbon are observed in both of the studied forms. Figure 5.a image also indicates that almost all of the formed particles in the carbon materials are linked together through the applied binder and subsequently a unified structure is created. The latter finding is consistent with the outcome of the obtained mechanical properties.[1] A comparison between Fig. 5.a and 5.b suggests that the size of structural macropores in the powder form becomes smaller after adding the binder mainly due to their compression and being transformed to partly-filled pores resulting in creation of structural mesopores.[1, 49] According to the BET analysis further discussed, the total surface area of the material decreases though the average pore size is enhanced by the addition of the binder.

On the other hand, the layered EDS image of sample G4 shown in Fig. 6 demonstrates that there are oxygen groups and phosphorus present on the carbon surface about which the distribution of phosphorus is uniform. On the basis of the relative information available in the literature, a support surface containing suitable amount and uniform dispersion of oxygen and phosphorus causes appropriate dispersion of active catalytic metals on its surface.[63]

Since the synthesized material G4 is supposed to be used as a support for the catalyst of a HDS process, it should be stable at elevated temperatures conventionally used in the corresponding operations (up to 400°C). Weight loss of the catalyst support brings about clumping of active phases and reducing its performance. For the purpose of testing the mentioned criterion, the synthetic activated carbon G4 was analyzed employing a TGA apparatus. According to Fig. 7, the weight of sample G4 decreases firstly by 5% at 100°C which is related to the evaporation of moisture in the sample.[64] Then, the main sudden weight loss begins at around 495°C due to decomposition of lignin content of the carbon source.[65, 66]

The reason for the increase in weight up to 495°C is related to the oxidation of the sample. In the sample G6, the weight of the activated carbon first increases by 10% up to 495°C. [30] The reason for this increase in weight is the oxidation of carbon groups, which causes even a percentage of weight to increase, but from 500°C and above, due to the destruction of carbon structures, the change in weight decreases. In another similar article related to palm trunk carbon, the weight in TGA analysis has increased up to 450°C.[67]

3.3. Mechanism of binder reaction

As pointed out earlier, the utilized binder impacts the synthesis process through a crosslink reaction. Figure 8 shows the proposed mechanism for such reaction involving citric acid and the CMC binder.

At high temperatures, the crosslinking agent dehydrates forming a cyclic anhydride. The formed anhydride then reacts with the CMC hydroxyls leading to the formation of ester bonds.[68, 69] The hydrogel polymeric structure is formed when the proposed mechanism occurs multiple times linking two different CMC chains.[70] Eventually, combination of the formed cellular groups and the citric acid group leads to creation of an organic structure, which is decomposed at high temperatures. Such decomposition left the carbons with mesoporous structure.[49] Consequently, the average pore size of a non-treated activated carbon increased from 2.8 to 5.6 nm due to the addition of citric acid (see Table 3). However, addition of coal tar pitch, blocks the mesopores during calcination. Within this context, addition of citric acid + CMC reduces blocking of active carbon pores.

3.4. Catalysts characterizations

The XRD patterns of the produced catalysts are shown in Fig. 9. Previously discussed, FeMo-G4 and FeMo-G6 stand for the catalysts made on the carbon supports of G4 and G6, respectively. The obtained peaks reveal presence of carbon and molybdenum oxide (MoO_3) crystals in the structure of the catalysts .[11] The peak related to molybdenum oxide is less intense in FeMo-G4 sample compared to the relevant peak observed for FeMo-G6 catalyst. Since, the synthetic activated carbon G4 has a higher average pore size than the commercial G6 material, the distribution of active metal particles in the former sample is more even than the latter material resulting in less intensity for the corresponding XRD peaks.[58]

Moreover, functional groups formed on the surface of the synthesized catalysts obtained by FTIR tests are reported in Fig. 10. The peaks at the wavelengths of 650 and 450 cm^{-1}, 940 and 880 cm^{-1}, and 600 and 450 cm^{-1} are corresponding to molybdenum trioxide (MoO_3), cis-molybdenum dioxide (cis-MoO_2) and hematite Fe_2O_3, respectively, which are consistent with the literature data.[13, 54] Other peaks in the wavelength ranges of 3750, 2350, 1530–1570, and 1060–1200 cm^{-1} are related to the functional groups of activated carbon.[56] On the other hand, comparison of the two catalysts indicates that intensities of the observed peaks are larger for the FeMo-G4 sample. This could indicate the higher acidity of the synthetic base catalyst, which is described in the TPD analysis section.

TPD analysis is used to measure the acidity of the surface of a material indicating the amount of weak and strong acids existing on the surface. The obtained results of the TPD analysis for samples synthesized in the present study are reported in Table 6. The total acidities of FeMo-G4 is 2.93 mmol/g ; while industrial carbon-based catalyst FeMo-G6 has a total acidities of 1.6 mmol/g. It is reported in the literature that there is a positive correlation between HDS catalysts activity and their surfaces acidity, which results in higher sulfur adsorption capacity on the surface of the catalyst. [58] According to Table 6, the amounts of total strong acids for samples FeMo-G4 is about the same at 0.37 mmol/g though the amounts of total weak acids. The difference between weak and strong acids on the surface is the amount of acids connected to the surface due to surface functionalization. The results are consistent

with the other findings reported in the literature stating that the activity of the used catalysts enhances by an increase in the amount of weak acid on the surface. [71]

Table 6
TPD results.

Catalysts	Total acidity (TPD) mmol/g catalyst		
	Weak acid	Strong acid	Weak/Strong acid
FeMo-G4	0.81	2.12	0.37
FeMo-G6	0.1	1.5	0.06

In order to investigate morphology of the produced catalyst with G4 sample as the support after sulfidation, a FESEM image was taken which is illustrated in Fig. 11. As can be seen, morphology of the FeMo-G4 catalyst shows low agglomeration of the particles through uniform dispersion of metal particles in its structure. But in the case of catalyst with commercial active carbon base, the percentage of accumulation is much higher, which indicates the lack of proper dispersion of active metals on the surface of the catalyst base. The reason for the better distribution of the catalyst on the synthetic active carbon base is due to the pore size of the support, because the larger mesopore size reduces the accumulation of catalyst particles on the support. [58]

The EDX photo is related to both catalysts after sulfidation. As can be seen in the Fig. 11, the distribution of metals in the FeMo-G4 catalyst is more uniform than the FeMo-G6 catalyst.

3.5. Performance of the catalysts

The HDS process for removal of the sulfur-bearing species existing in a heavy naphtha sample was operated using the apparatus shown in Fig. 12. The output results of such process, reported in Fig. 12, can help evaluate the performance of the two synthesized catalysts at atmospheric pressure. To get the best reaction conditions. The reaction was carried out at different temperatures and different LHSVs. Then, the reaction was carried out in optimal conditions at different times to measure the stability of the catalyst and the time on stream (TOS) diagram was drawn. It is inferred from the results that conversion of the sulfur-containing compounds using FeMo-G4 catalyst at 340°C and 1 bar becomes stable at 80% after 6 hours while maximum conversion percentage is around 66% utilizing the FeMo-G6 catalyst. The obtained results also reveal higher efficiency of the synthesized FeMo-G4 catalyst for sulfur removal at atmospheric conditions compared to the catalysts tested in the literature.[72, 73] Another point worth to be mentioned here is that the produced catalyst of FeMo-G4 in this work contains Fe promoter metal in its structure which makes it an economically viable catalyst for industrial production compared to the existing catalysts comprising more expensive active metals.[74]

In addition, to compare the catalytic performance of the hydrotreating reaction of fuel reported in the literature, Table 7 lists the results of a series of studies in this regard. Comparing the work done with the previous work[31] shows that granulation not only did not lower the performance of the catalyst but also led to the improvement of the performance of the catalyst. The reason for that can be pointed to the good choice of binders and the increase in the size of mesopores during granulation.

The catalyst synthesized in this study has improved significantly in terms of chemical, physical and functional characteristics compared to previous catalysts. The results show the superiority of the catalyst and the basis of the present catalyst.

Table 7
Comparison of the HDS of fuel .

Catalyst	Feed	Pressure (bar)	Temperature (°C)	Conversion	Ref
FeMo-AC (powder) 8% Mo, 2–3%Fe	Heavy naphtha	1	340	78	Soleymani et al[31]
pt-Al_2O_3 %5.7	Commercial low sulfur diesel 508	1	290 350	60.9 65.4	Haji et al[47]
FeMo-AC 9.2%Mo, 1.9%Fe	Thiophen	1	350	68	Ramselaar et al [73]
FeMo-Al_2O_3 12%Mo,Fe(< 1%)	Thiophen	1	350	24	Kraleva et al[72]
FeMo-AC(G4) (Granular) 8% Mo, 2–3%Fe	Heavy naphtha	1	340	80	This study

4. Conclusions

In this research, the main goal was to synthesize a mesoporous activated carbon with high mechanical strength. For this purpose, a soft template was used to create the mesoporous structure of carbon. Furthermore, use of a combination of three binder materials including coal tar pitch, citric acid, and carboxymethylcellulose (CMC) led to achieve optimal values of the desirable properties of the carbon as follows:

- The crush strength = 276 N/cm;
- Specific surface area = 950 m^2/g
- Average pore size = 5.6 nm
- Mesopore volume/total pore volume = 92%

In the final step of the study, performance of the phosphorus-doped mesoporous activated carbon to be used as a support of a HDS process catalyst was experimentally tested. The studied sulfur-bearing material was a heavy naphtha sample containing 900 ppm total sulfur. The obtained results indicated that the sulfur conversion applying the FeMo catalyst synthesized with the phosphorus-doped activated carbon support was around 80 % at 340°C and 1 bar, while the produced catalyst based on a commercial activated carbon resulted in 66 % conversion for the same operation.

Declarations

Author Contribution

A- The main author and researcher and draw the graphs and tables and analyzesB- The first instructorC- The second instructord- text editing

Acknowledgments

The authors are grateful to the Research Institute of Petroleum Industry [RIPI], and the Iran National Since Foundation [INSF] for their support of this work.

Declaration of interests

The authors declare the following financial interests which may be considered as potential competing interests:

The authors are grateful to the Iran National Since Foundation [INSF] for their support of this work.

References

1. Yue, Z., Economy, J.: Synthesis of highly mesoporous carbon pellets from carbon black and polymer binder by chemical activation. Microporous Mesoporous Mater. **96**(1–3), 314–320 (2006)
2. Moosavi, E.S., Rezaei, N., Karimzadeh, R.: Numerical computer algorithm for pore size distribution analysis of activated carbons based on local density functional theory. Can. J. Chem. Eng. **92**(10), 1739–1748 (2014)

3. Moosavi, E.S., Dastgheib, S.A., Karimzadeh, R.: Adsorption of thiophenic compounds from model diesel fuel using copper and nickel impregnated activated carbons. Energies. **5**(10), 4233–4250 (2012)
4. Moosavi, E.S., Karimzadeh, R.: Adsorption of thiophenic compounds by OFG-tailored fiber and activated carbons. Sep. Sci. Technol. **50**(13), 1940–1951 (2015)
5. Han, S., Kim, S., Lim, H., Choi, W., Park, H., Yoon, J., Hyeon, T.: New nanoporous carbon materials with high adsorption capacity and rapid adsorption kinetics for removing humic acids. Microporous Mesoporous Mater. **58**(2), 131–135 (2003)
6. Li, Q., Snoeyink, V.L., Mariñas, B.J., Campos, C.: Pore blockage effect of NOM on atrazine adsorption kinetics of PAC: the roles of PAC pore size distribution and NOM molecular weight. Water Res. **37**(20), 4863–4872 (2003)
7. Hartmann, M., Vinu, A., Chandrasekar, A.: G Chem. Mater. **17**, 829 (2005)
8. Tehrani, N.H.M.H., Alivand, M.S., Maklavany, D.M., Rashidi, A., Samipoorgiri, M., Seif, A., Yousefian, Z.: Novel asphaltene-derived nanoporous carbon with NS-rich micro-mesoporous structure for superior gas adsorption: Experimental and DFT study. Chem. Eng. J. **358**, 1126–1138 (2019)
9. Moradi, S., Moosavi, E., Karimzadeh, R.: Stability Determination of the Modified Activated Carbon to Adsorb Thiophenic Compounds from Model Diesel Fuel. Iran. J. Chem. Chem. Eng. **38**(4), 149–165 (2019)
10. Abrahamson, J.P.: Effects of Catalyst Properties on Hydrodesulfurization on of Fluid Catalytic Cracking Decant Oils as Feedstock for Needle Coke. (2015)
11. Kohli, K., Prajapati, R., Maity, S.K., Sharma, B.K.: Effect of silica, activated carbon, and alumina supports on NiMo catalysts for residue upgrading. Energies. **13**(18), 4967 (2020)
12. Duchet, J., Van Oers, E., De Beer, V., Prins, R.: Carbon-supported sulfide catalysts. J. Catal. **80**(2), 386–402 (1983)
13. Hajjar, Z., Kazemeini, M., Rashidi, A., Soltanali, S.: Hydrodesulfurization catalysts based on carbon nanostructures: A review. Fullerenes Nanotubes Carbon Nanostruct. **26**(9), 557–569 (2018)
14. Wang, B., Chen, Z., Jiang, T., Yu, J., Yang, H., Duan, A., Xu, C.: Comparison of the intraparticle diffusion of DBT and 4, 6-DMDBT in HDS over different mesostructured silica-based catalysts. Fuel. **324**, 124516 (2022)
15. Motejadded Emrooz, H.B., Maleki, M., Rashidi, A., Shokouhimehr, M.: Adsorption mechanism of a cationic dye on a biomass-derived micro-and mesoporous carbon: structural, kinetic, and equilibrium insight. Biomass Convers. Biorefinery. **11**, 943–954 (2021)
16. Abotsi, G.M., Scaroni, A.W.: A review of carbon-supported hydrodesulfurization catalysts. Fuel Process. Technol. **22**(2), 107–133 (1989)
17. de Beer, V.H., Derbyshire, F.J., Groot, C.K., Prins, R., Scaroni, A.W., Solar, J.M.: Hydrodesulphurization activity and coking propensity of carbon and alumina supported catalysts. Fuel. **63**(8), 1095–1100 (1984)

18. Kaluža, L., Gulková, D., Vít, Z., Zdražil, M.: Effect of support type on the magnitude of synergism and promotion in CoMo sulphide hydrodesulphurisation catalyst. Appl. Catal. A. **324**, 30–35 (2007)
19. Kouzu, M., Kuriki, Y., Uchida, K., Sakanishi, K., Sugimoto, Y., Saito, I., Fujii, D., Hirano, K.: Catalytic Hydrocracking of Petroleum Residue over Carbon-Supported Nickel – Molybdenum Sulfides. Energy fuels. **19**(3), 725–730 (2005)
20. Hajjar, Z., Kazemeini, M., Rashidi, A., Soltanali, S.: Optimizing parameters affecting synthesis of a novel Co–Mo/GO catalyst in a Naphtha HDS reaction utilizing D-optimal experimental design method. J. Taiwan Inst. Chem. Eng. **78**, 566–575 (2017)
21. Joshi, Y.V., Ghosh, P., Daage, M., Delgass, W.N.: Support effects in HDS catalysts: DFT analysis of thiolysis and hydrolysis energies of metal–support linkages. J. Catal. **257**(1), 71–80 (2008)
22. Farag, H.: Synthesis of CoMo-based carbon hydrodesulfurization catalysts: Influence of the order of metal impregnations on the activity. Appl. Catal. B. **84**(1–2), 1–8 (2008)
23. Matos, J., Brito, J.L., Laine, J.: Activated carbon supported Ni Mo: effects of pretreatment and composition on catalyst reducibility and on ethylene conversion. Appl. Catal. A. **152**(1), 27–42 (1997)
24. Hubaut, R., Altafulla, J., Rives, A., Scott, C.: Characterization and HDS activities of mixed Fe–Mo sulphides supported on alumina and carbon. Fuel. **86**(5–6), 743–749 (2007)
25. Farag, H., Whitehurst, D., Sakanishi, K., Mochida, I.: Carbon versus alumina as a support for Co–Mo catalysts reactivity towards HDS of dibenzothiophenes and diesel fuel. Catal. Today. **50**(1), 9–17 (1999)
26. Guojun, S., Yu, Z., Jianyi, S.: Mesoporous carbon supported Co-Mo and Ni-Mo catalysts for hydrodesulfurization. Chin. J. Catal. **31**(8), 961–964 (2010)
27. Hu, S., Zuo, S., Xu, Z., Han, C., Shen, J.: Mesoporous carbon materials prepared from carbohydrates with a metal chloride template. J. Mater. Chem. **19**(41), 7759–7764 (2009)
28. Saleh, T.A., Danmaliki, G.I.: Influence of acidic and basic treatments of activated carbon derived from waste rubber tires on adsorptive desulfurization of thiophenes. J. Taiwan Inst. Chem. Eng. **60**, 460–468 (2016)
29. Abubakar, U.C., Alhooshani, K.R., Adamu, S., Al Thagfi, J., Saleh, T.A.: The effect of calcination temperature on the activity of hydrodesulfurization catalysts supported on mesoporous activated carbon. J. Clean. Prod. **211**, 1567–1575 (2019)
30. Soleymani, M., Karimzadeh, R., Rashidi, A., Eslamimanesh, A.: Effectiveness Study of Mesoporous Size, Acidity, and Precursor Type on Characterization of Activated Carbon as an Fe–Mo Catalyst Support for Hydrodesulfurization of Heavy Naphtha. Industrial & Engineering Chemistry Research (2023)
31. Soleymani, M., Karimzadeh, R., Rashidi, A., Eslamimanesh, A.: Effectiveness Study of Mesoporous Size, Acidity, and Precursor Type on Characterization of Activated Carbon as an Fe–Mo Catalyst Support for Hydrodesulfurization of Heavy Naphtha. Ind. Eng. Chem. Res. **62**(27), 10419–10430 (2023)

32. Sharifi, K., Halladj, R., Royaee, S.J., Nasr, M.: Investigation of the effect of HZSM-5 over HDS and reforming processes for clean gasoline production. Int. J. Environ. Sci. Technol. **16**(2), 865–874 (2019)
33. Bajwa, A., Moraga, F., Balakrishnan, M., Svensson, G., Batra, V.S.: Activated carbon monoliths by pressureless technique for environmental applications. Environ. Prog. Sustain. Energy. **34**(5), 1420–1426 (2015)
34. Zong, Y., Zhang, Y., Lin, X., Ye, D., Qiao, D., Zeng, S.: Facile synthesis of potassium copper ferrocyanide composite particles for selective cesium removal from wastewater in the batch and continuous processes. RSC Adv. **7**(50), 31352–31364 (2017)
35. Li, J., Zhuang, N., Xie, J., Zhu, Y., Lai, H., Qin, W., Javed, M.S., Xie, W., Mai, W.: Carboxymethyl cellulose binder greatly stabilizes porous hollow carbon submicrospheres in capacitive K-ion storage. ACS Appl. Mater. Interfaces. **11**(17), 15581–15590 (2019)
36. Mian, M.M., Kamana, I.M.L., An, X., Abbas, S.C., Ahommed, M.S., He, Z., Ni, Y.: Cellulose nanofibers as effective binders for activated biochar-derived high-performance supercapacitors. Carbohydr. Polym. **301**, 120353 (2023)
37. Rocha, V., Blanco, C., Santamaría, R., Diestre, E., Menéndez, R., Granda, M.: Pitch/coke wetting behaviour. Fuel. **84**(12–13), 1550–1556 (2005)
38. Sarkar, A., Kocaefe, D., Kocaefe, Y., Sarkar, D., Bhattacharyay, D., Morais, B., Chabot, J.: Coke–pitch interactions during anode preparation. Fuel. **117**, 598–607 (2014)
39. Lu, Y., Kocaefe, D., Kocaefe, Y., Huang, X.-A., Bhattacharyay, D.: The wettability of coke by pitches with different quinoline-insoluble contents. Fuel. **199**, 587–597 (2017)
40. Monsen, B., Ratvik, A., Lossius, L.: Charcoal in anodes for aluminium production. Minerals, Metals and Materials Society/AIME, 420 Commonwealth Dr., P. O. Box &#8230
41. Hussein, A., Fafard, M., Ziegler, D., Alamdari, H.: Effects of charcoal addition on the properties of carbon anodes. Metals. **7**(3), 98 (2017)
42. Tian, B., Li, P., Li, D., Qiao, Y., Xu, D., Tian, Y.: Preparation of micro-porous monolithic activated carbon from anthracite coal using coal tar pitch as binder. J. Porous Mater. **25**, 989–997 (2018)
43. Columnar activated carbon based on: coal pitch binders and preparation method of columnar activated carbon. CN102674341A (2012)
44. Columnar activated carbon based on: coal pitch binders and preparation method of columnar activated carbon. **CN102674341A**, -09–19. (2012)
45. Hamasaki, A., Furuse, A., Sekinuma, Y., Fujio, K., Iide, M., Ozeki, S.: Improving the micropore capacity of activated carbon by preparation under a high magnetic field of 10 T. Sci. Rep. **9**(1), 1–11 (2019)
46. Gao, S., Ge, L., Rufford, T.E., Zhu, Z.: The preparation of activated carbon discs from tar pitch and coal powder for adsorption of CO2, CH4 and N2. Microporous Mesoporous Mater. **238**, 19–26 (2017)
47. Higai, D., Huang, Z., Qian, E.W.: Preparation and surface characteristics of phosphoric acid-activated carbon from coconut shell in air. Environ. Prog. Sustain. Energy **40** (2), e13509. (2021)

48. Laszlo Domokos, H.J., kindJohannes: Van Veen Catalyst composition preparation and use. US20040182749A1, (2004)
49. Rashidi, A., Akbarnejad, M., Khodadadi, A., Mortazavi, Y., Ahmadpourd, A.: Single-wall carbon nanotubes synthesized using organic additives to Co–Mo catalysts supported on nanoporous MgO. Nanotechnology. **18**(31), 315605 (2007)
50. Lim, A., Chew, J.J., Ngu, L.H., Ismadji, S., Khaerudini, D.S., Sunarso, J.: Synthesis, characterization, adsorption isotherm, and kinetic study of oil palm trunk-derived activated carbon for tannin removal from aqueous solution. ACS omega. **5**(44), 28673–28683 (2020)
51. Moyo, M., Nyamhere, G., Sebata, E., Guyo, U.: Kinetic and equilibrium modelling of lead sorption from aqueous solution by activated carbon from goat dung. Desalination Water Treat. **57**(2), 765–775 (2016)
52. Xie, Z., Guan, W., Ji, F., Song, Z., Zhao, Y.: Production of biologically activated carbon from orange peel and landfill leachate subsequent treatment technology. *Journal of chemistry 2014*. (2014)
53. Kristianto, H., Arie, A.A., Susanti, R.F., Halim, M., Lee, J.: In *The effect of activated carbon support surface modification on characteristics of carbon nanospheres prepared by deposition precipitation of Fe-catalyst*, IOP Conference Series: Materials Science and Engineering, IOP Publishing: ; p 012034. (2016)
54. Fang, N., Ji, Y.-M., Li, C.-Y., Wu, Y.-Y., Ma, C.-G., Liu, H.-L., Li, M.-X.: Synthesis and adsorption properties of [Cu (L) 2 (H 2 O)] H 2 [Cu (L) 2 (P 2 Mo 5 O 23)]· 4H 2 O/Fe 3 O 4 nanocomposites. RSC Adv. **7**(41), 25325–25333 (2017)
55. Kaluža, L., Palcheva, R., Spojakina, A., Jirátová, K., Tyuliev, G.: Hydrodesulfurization NiMo catalysts supported on Co, Ni and B modified Al2O3 from Anderson heteropolymolybdates. Procedia Eng. **42**, 873–884 (2012)
56. Shrestha, D., Maensiri, S., Wongpratat, U., Lee, S.W., Nyachhyon, A.R.: Shorea robusta derived activated carbon decorated with manganese dioxide hybrid composite for improved capacitive behaviors. J. Environ. Chem. Eng. **7**(5), 103227 (2019)
57. Huang, C.-C., Li, H.-S., Chen, C.-H.: Effect of surface acidic oxides of activated carbon on adsorption of ammonia. J. Hazard. Mater. **159**(2–3), 523–527 (2008)
58. Lubis, S., Ramli, M., Ermanda, Y.: In *Hydrothermal Synthesis of Activated Carbon/α-Fe2O3 Nanocomposite and Its Application for Removing Tartrazine Dye*, IOP Conference Series: Materials Science and Engineering, IOP Publishing: ; p 012061. (2020)
59. Ang, T.N., Young, B.R., Taylor, M., Burrell, R., Aroua, M.K., Chen, W.-H., Baroutian, S.: Enrichment of surface oxygen functionalities on activated carbon for adsorptive removal of sevoflurane. Chemosphere. **260**, 127496 (2020)
60. Brennan, J.K., Thomson, K.T., Gubbins, K.E.: Adsorption of water in activated carbons: effects of pore blocking and connectivity. Langmuir. **18**(14), 5438–5447 (2002)
61. Soltanali, S., Mashayekhi, M., Mohaddecy, S.R.S.: Comprehensive investigation of the effect of adding phosphorus and/or boron to NiMo/γ-Al2O3 catalyst in diesel fuel hydrotreating. Process Saf.

Environ. Prot. **137**, 273–281 (2020)

62. Li, J., Hou, X., Mao, Y., Lai, C., Yuan, X.: Enhanced Performance of Aprotic Electrolyte Li–O2 Batteries with SnS2–SnO2/C Heterostructure as Efficient Cathode Catalyst. Energy Fuels. **34**(11), 14995–15003 (2020)
63. Xiao, C., Zheng, P., Shi, Y., Hu, D., Mei, J., Wang, G., Duan, A., Jiang, G., Liu, J.: Phosphoric acid modified Al-TUD-1 material to enhance hydrodesulfurization activities of dibenzothiophene and FCC diesel. Catal. Today. **374**, 154–161 (2021)
64. Suarez-Ojeda, M.E., Stüber, F., Fortuny, A., Fabregat, A., Carrera, J., Font, J.: Catalytic wet air oxidation of substituted phenols using activated carbon as catalyst. Appl. Catal. B. **58**(1–2), 105–114 (2005)
65. Basheer, O., Hanafiah, A.M., Abdulhakim Alsaadi, M., Al-Douri, M., Malek, Y., Mohammed Aljumaily, M., Saadi Fiyadh, M.: Synthesis and characterization of natural extracted precursor date palm fibre-based activated carbon for aluminum removal by RSM optimization. Processes. **7**(5), 249 (2019)
66. Hsieh, P.-F., Wen, T.-Y.: Evaluation of ozone removal by spent coffee grounds. Sci. Rep. **10**(1), 1–8 (2020)
67. Maryam, M., Abu Bakar, S., Shamsudin, M., Rusop Mahmood, M.: Synthesis of carbon nanotubes from palm oil precursor by aerosol-assisted catalytic CVD method. Appl. Mech. Mater. **229**, 247–251 (2012)
68. Ayouch, I., Kassem, I., Kassab, Z., Barrak, I., Barhoun, A., Jacquemin, J., Draoui, K., El Achaby, M.: Crosslinked carboxymethyl cellulose-hydroxyethyl cellulose hydrogel films for adsorption of cadmium and methylene blue from aqueous solutions. Surf. Interfaces. **24**, 101124 (2021)
69. Mali, K., Dhawale, S., Dias, R., Dhane, N., Ghorpade, V.: Citric acid crosslinked carboxymethyl cellulose-based composite hydrogel films for drug delivery. Indian J. Pharm. Sci. **80**(4), 657–667 (2018)
70. de Lima, G.F., de Souza, A.G., Rosa, D.: d. S. In *Nanocellulose as reinforcement in carboxymethylcellulose superabsorbent nanocomposite hydrogels*, Macromolecular Symposia, Wiley Online Library: ; p 2000126. (2020)
71. Cao, Z., Zhang, X., Guo, R., Ding, S., Zheng, P., Fan, J., Mei, J., Xu, C., Duan, A.: Synergistic effect of acidity and active phases for NiMo catalysts on dibenzothiophene hydrodesulfurization performance. Chem. Eng. J. **400**, 125886 (2020)
72. Kraleva, E., Spojakina, A., Jiratova, K., Petrov, L.: Support effect on the properties of iron–molybdenum hydrodesulfurization catalysts. Catal. Lett. **112**, 203–212 (2006)
73. Ramselaar, W., Crajé, M., Gerkema, E., De Beer, V., van Der Kraan, A.: An In-Situ Mössbauer Study on the Formation and Stability of the Fe-Mo-S Phase in Carbon-Supported Iron Molybdenum Sulfide Hds Catalysts. Bull. des. Sociétés Chimiques Belges. **96**(11–12), 931–940 (1987)
74. Li, H., Liu, J., Li, J., Hu, Y., Wang, W., Yuan, D., Wang, Y., Yang, T., Li, L., Sun, H.: Promotion of the inactive iron sulfide to an efficient hydrodesulfurization catalyst. ACS Catal. **7**(7), 4805–4816 (2017)

Figures

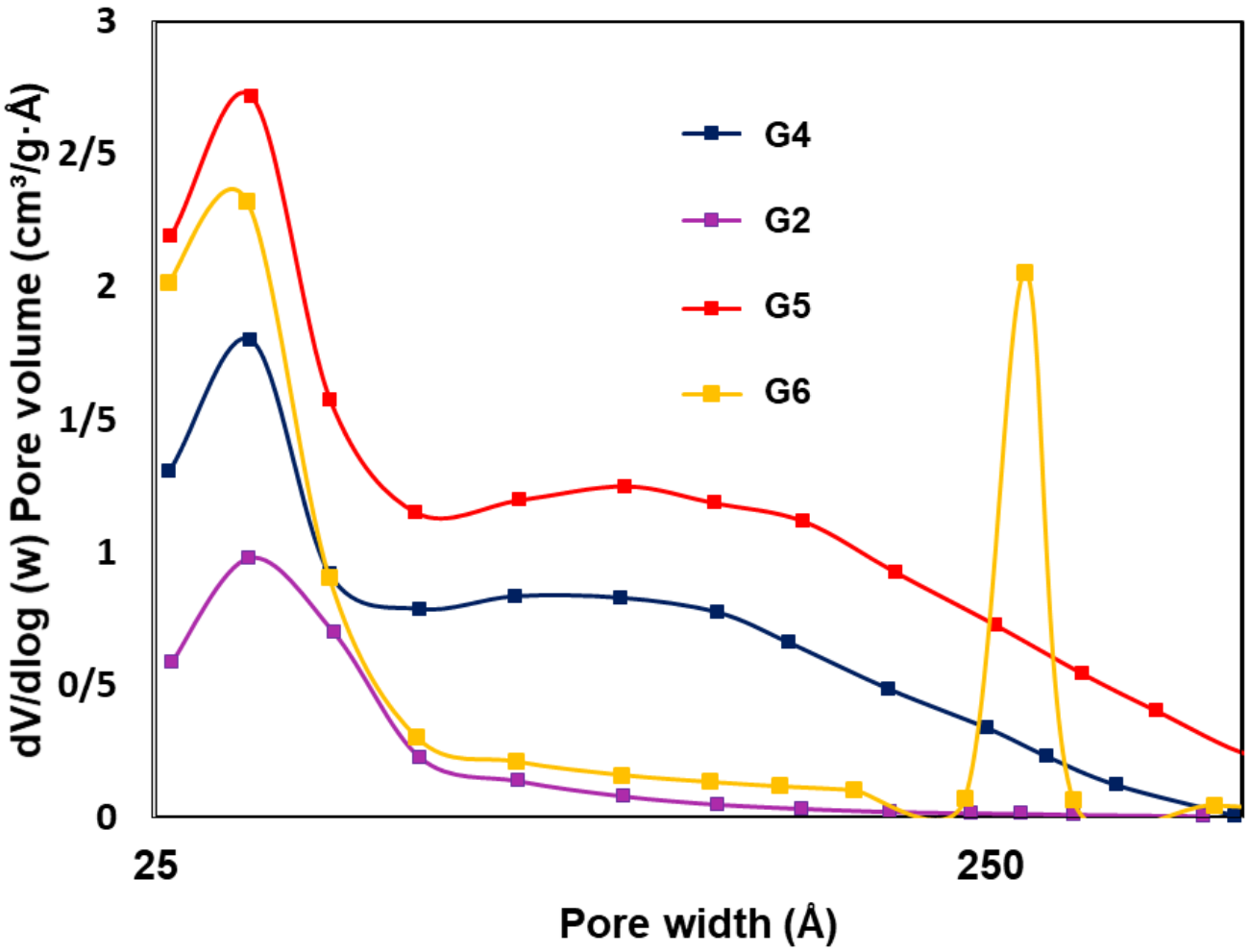

Figure 1

BJH pore size distribution graphs of granular activated carbons.

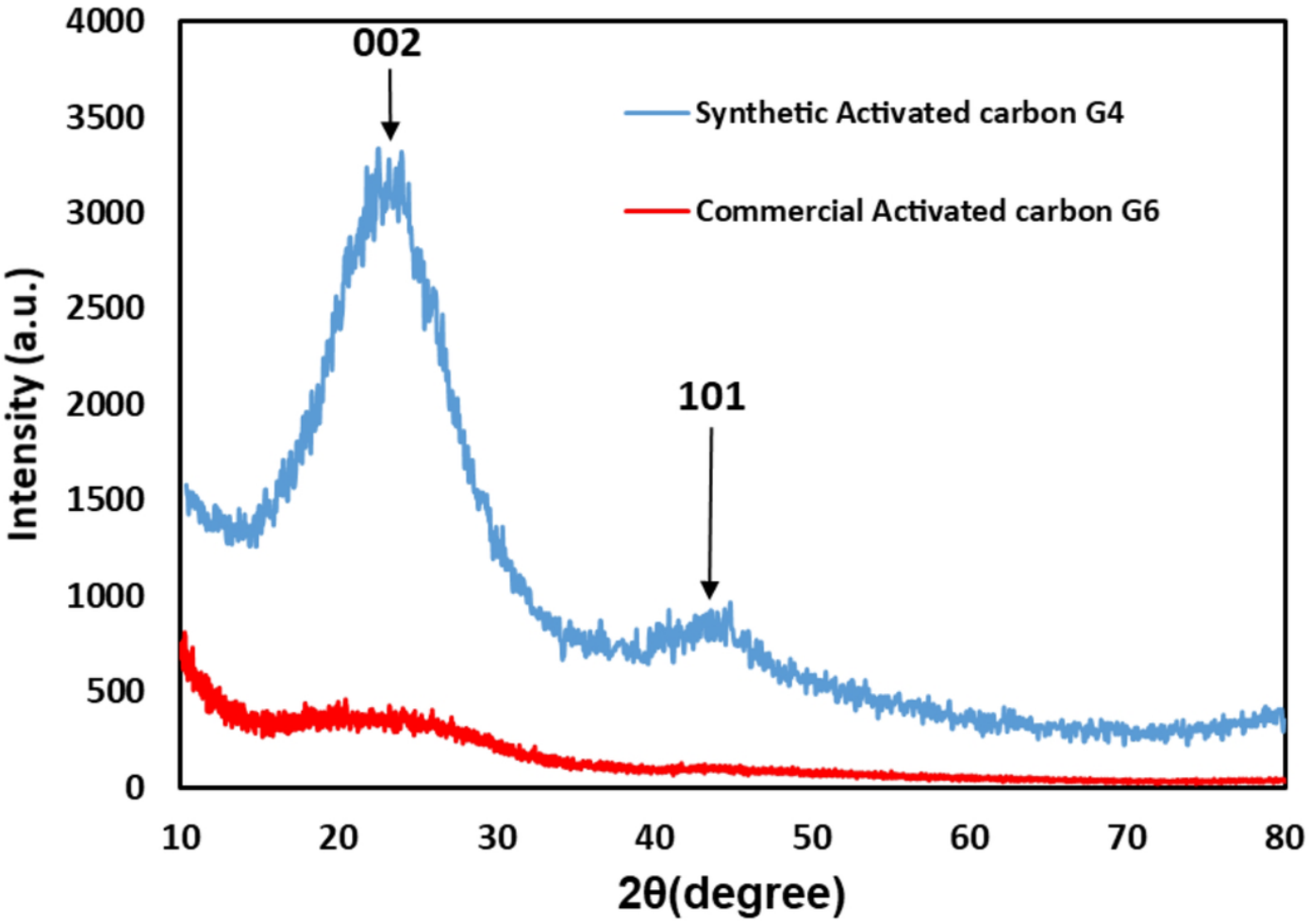

Figure 2

XRD pattern of synthetic granular AC (G4), and commercial activated carbon.

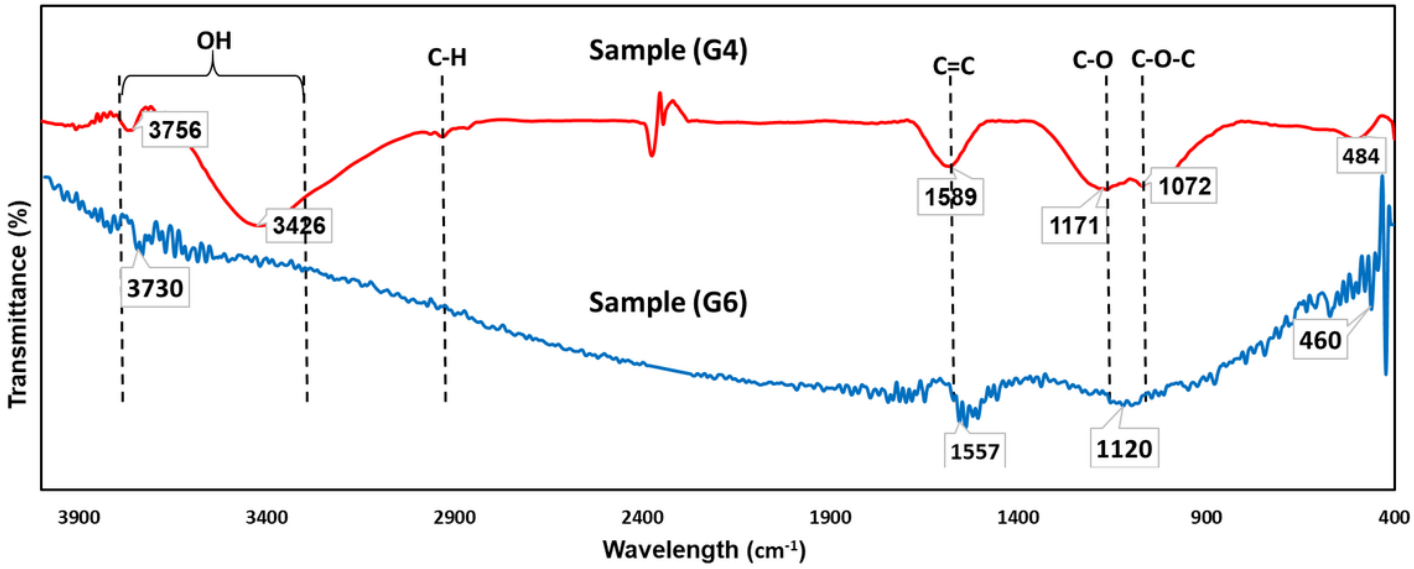

Figure 3

FTIR spectra of the synthesized and commercial AC samples.

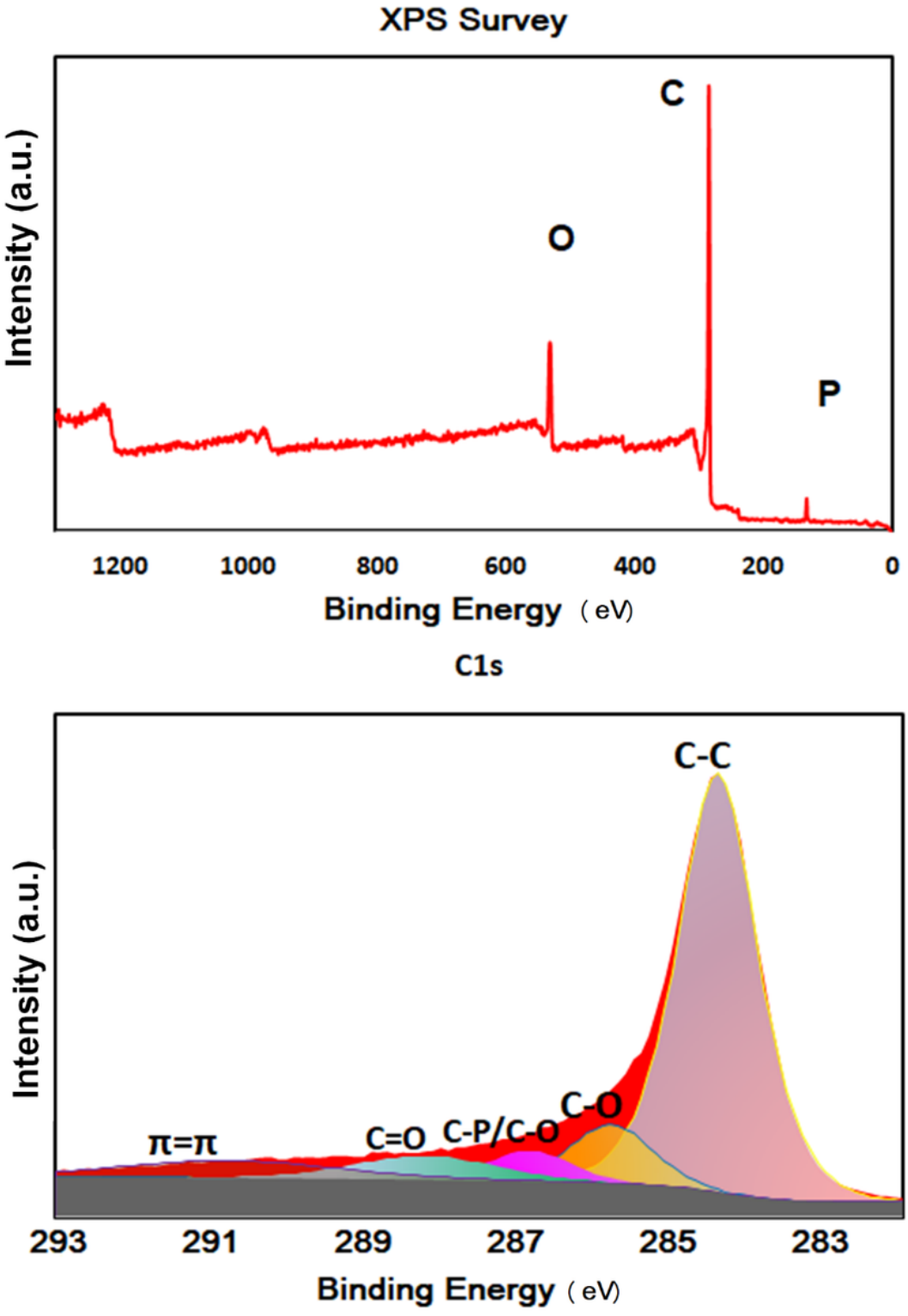

Figure 4

XPS analyses of the synthesized activated carbon (G4).

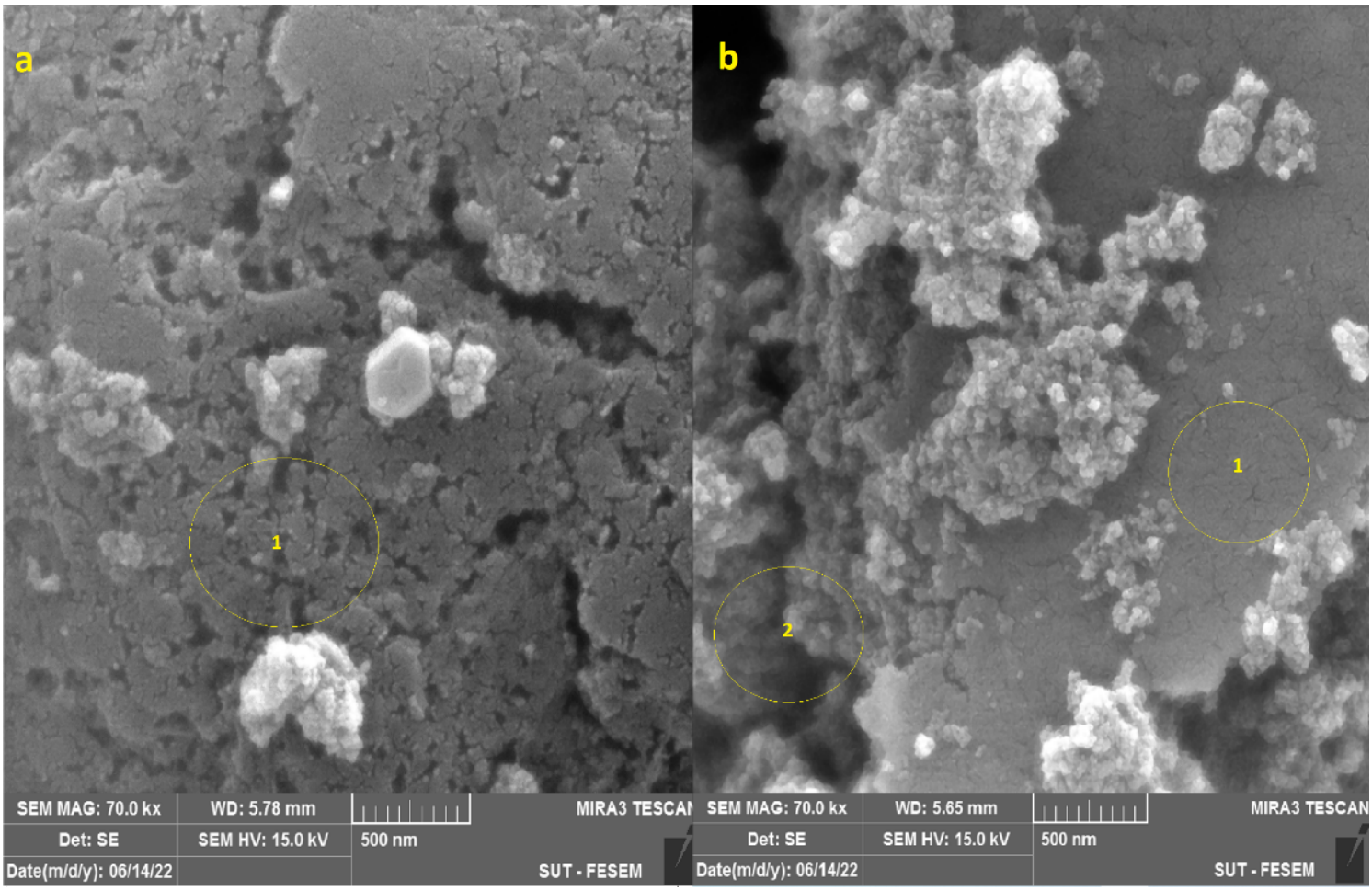

Figure 5

Effect of granulation on the pore structures of synthetic activated carbons a) Sample G1; b) Sample G4.

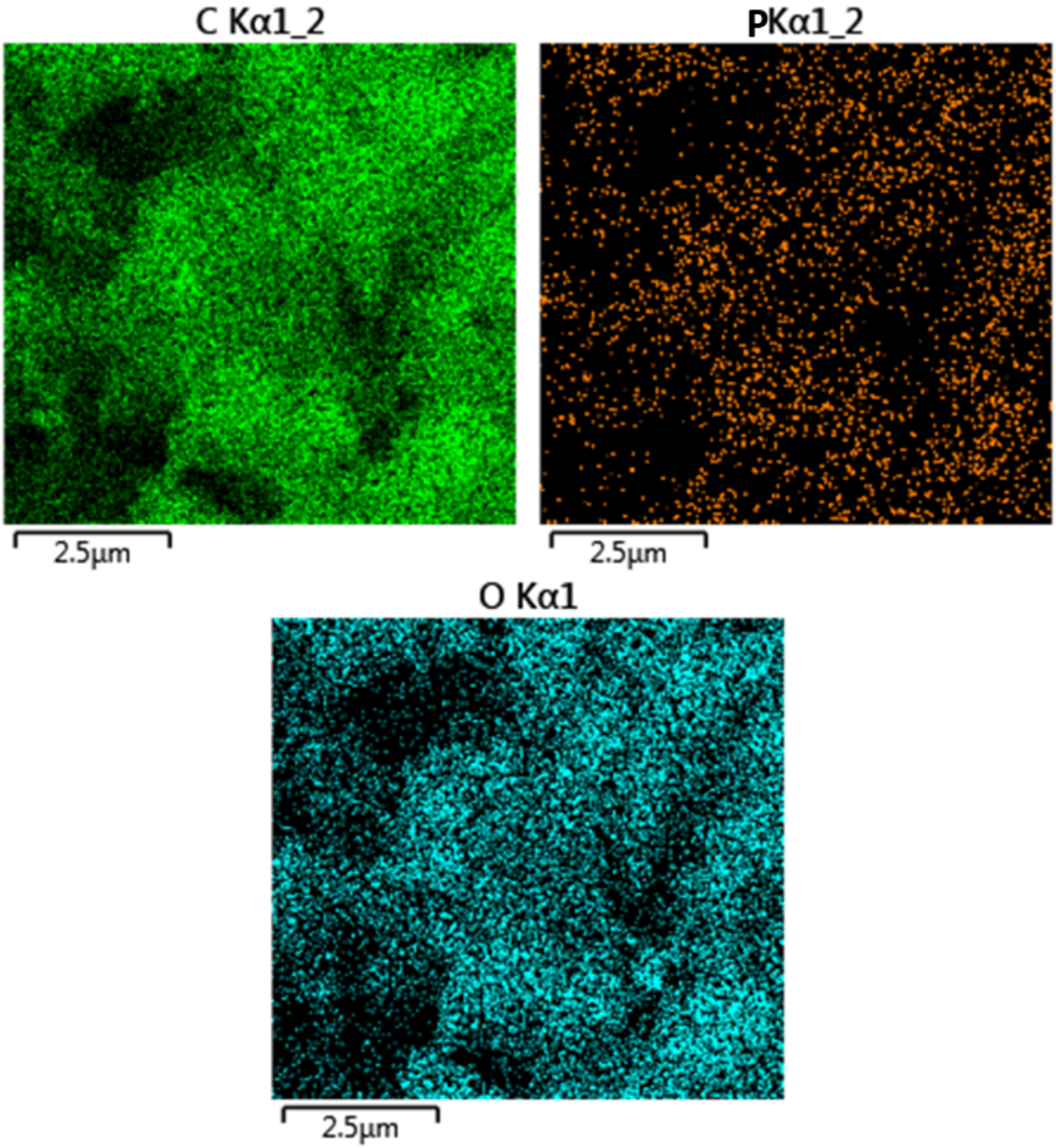

Figure 6

EDX images of synthetic activated carbon (G4).

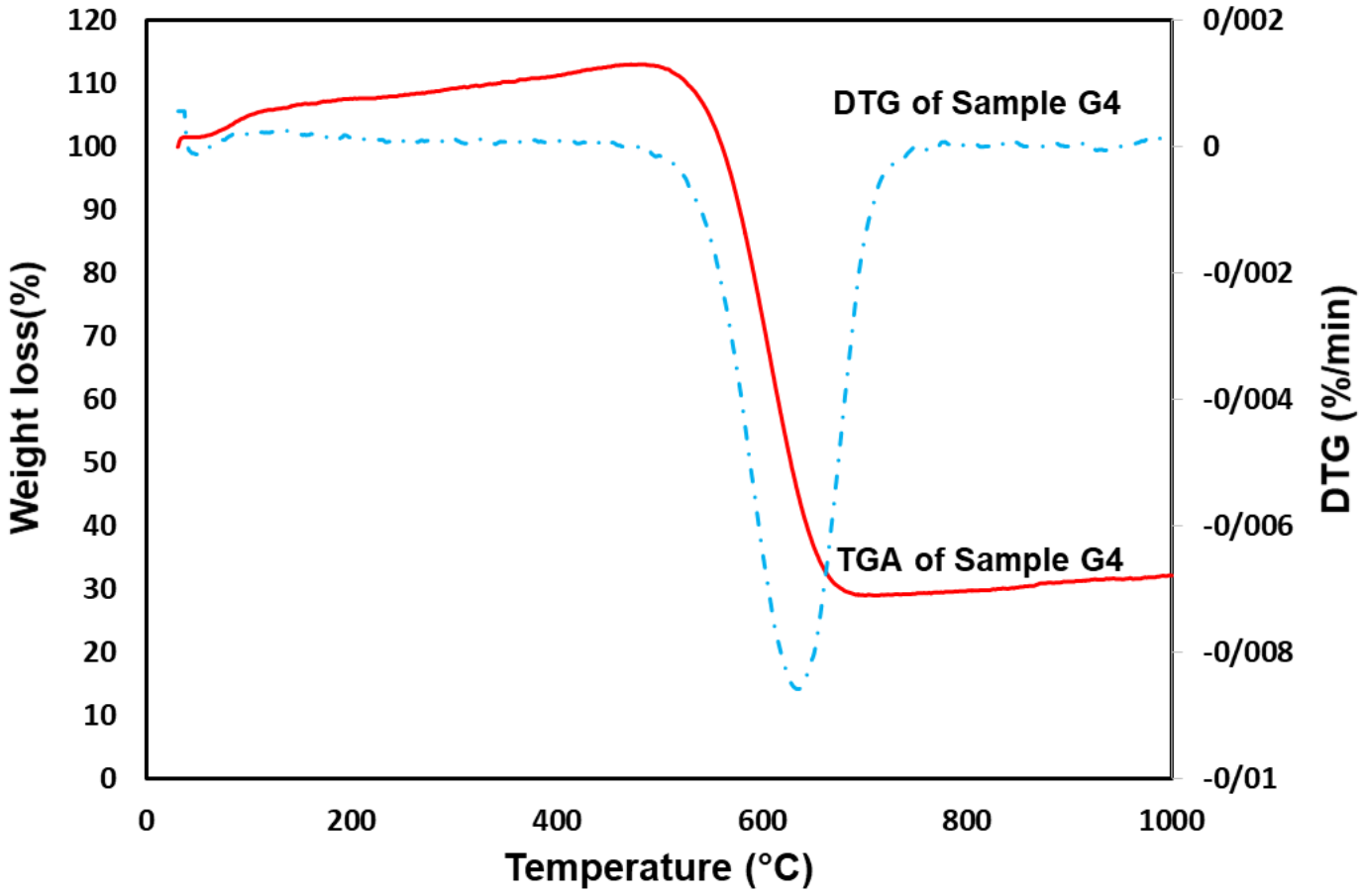

Figure 7

TGA analysis of the synthesized G4 sample.

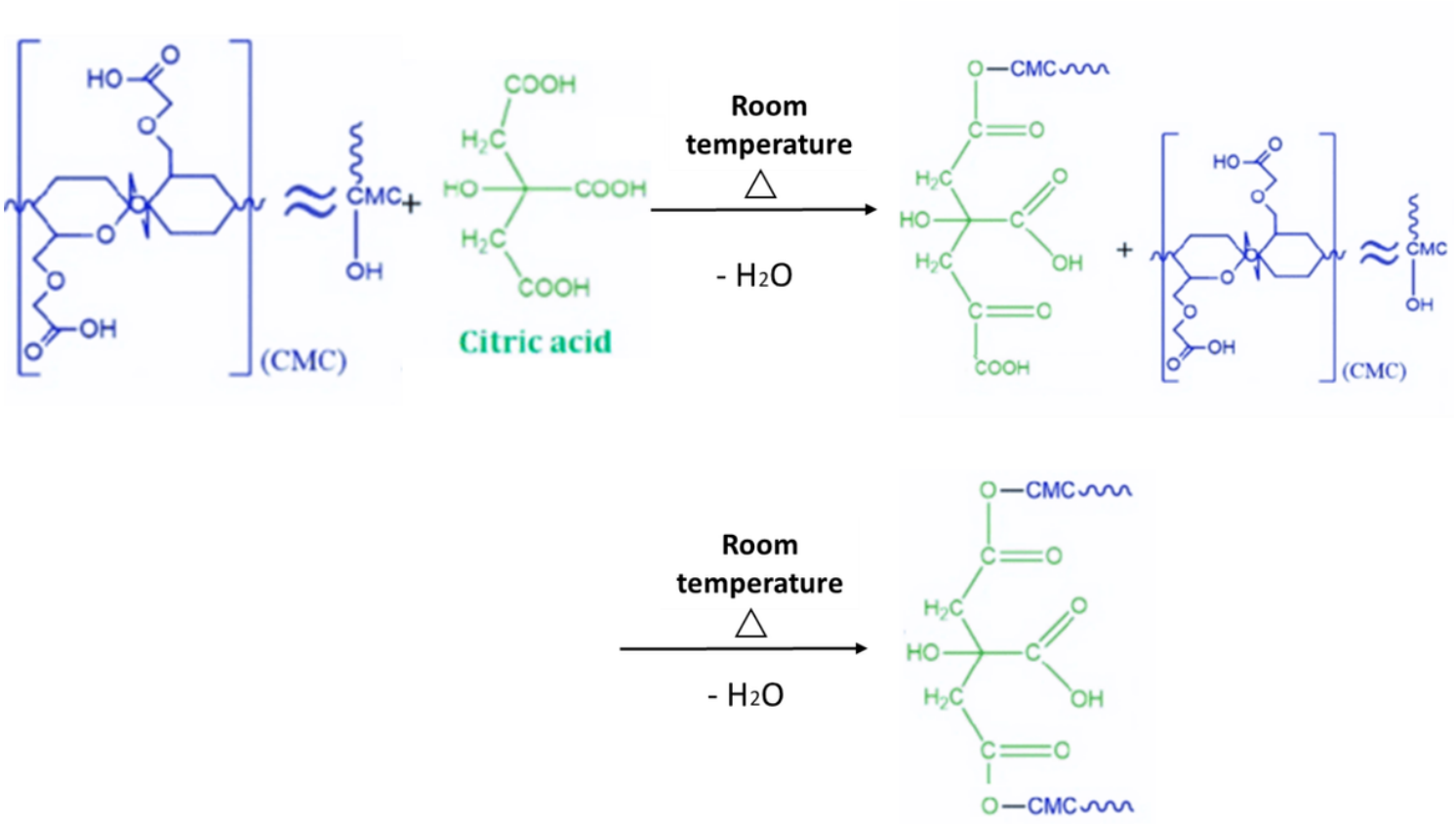

Figure 8

The mechanism of the crosslink reaction of the CMC hydrogel with citric acid

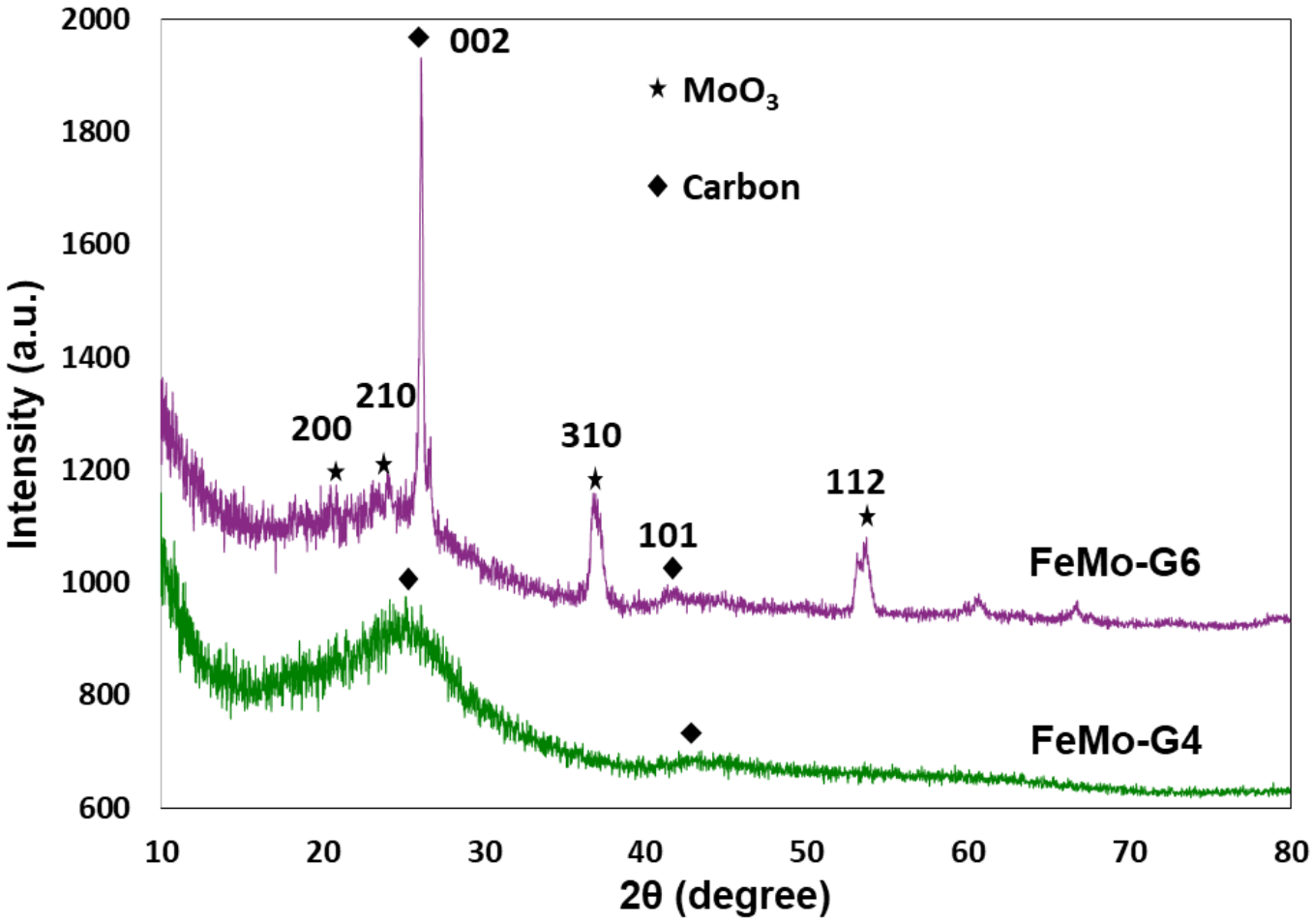

Figure 9

The obtained XRD peaks for the produced catalysts in this work.

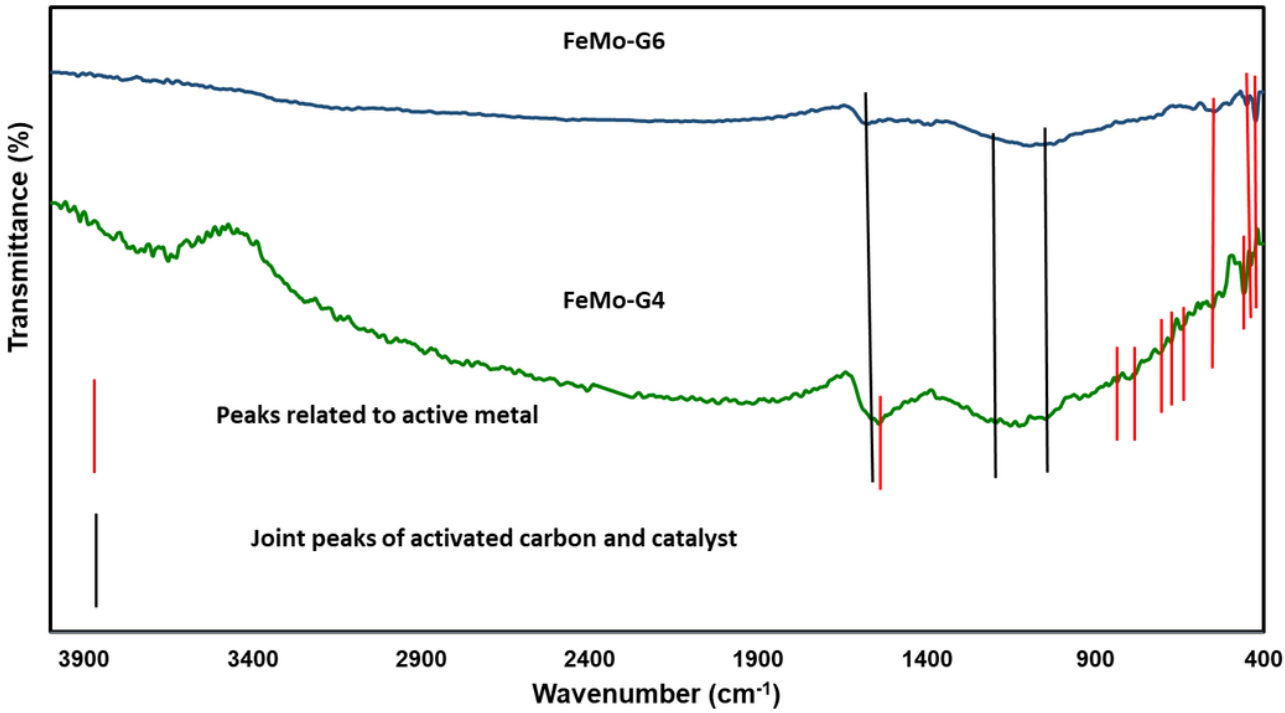

Figure 10

FTIR analyses of the catalysts.

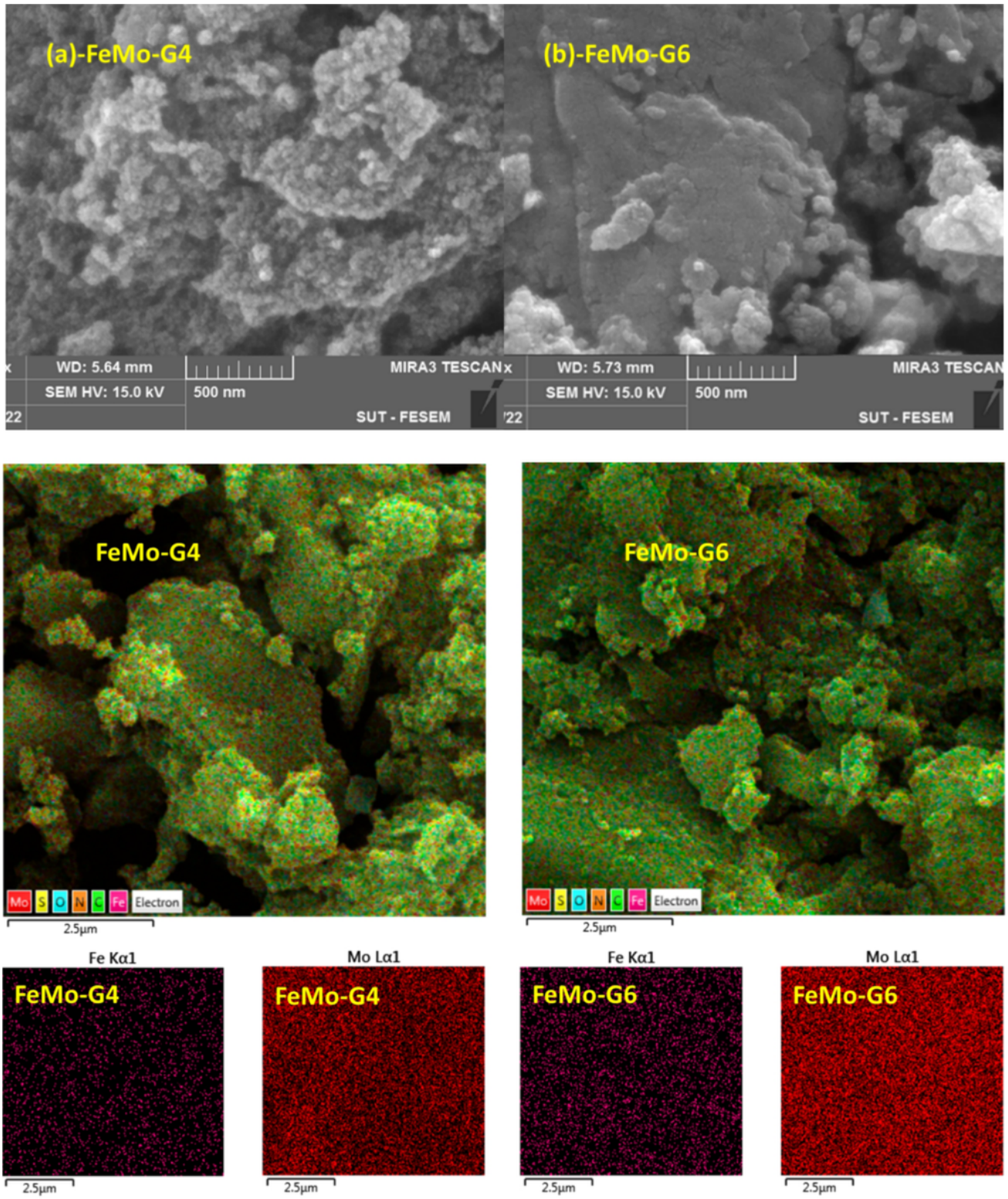

Figure 11

FESEM and EDS image of a- FeMo-G4 and b- FeMo-G6 catalysts.

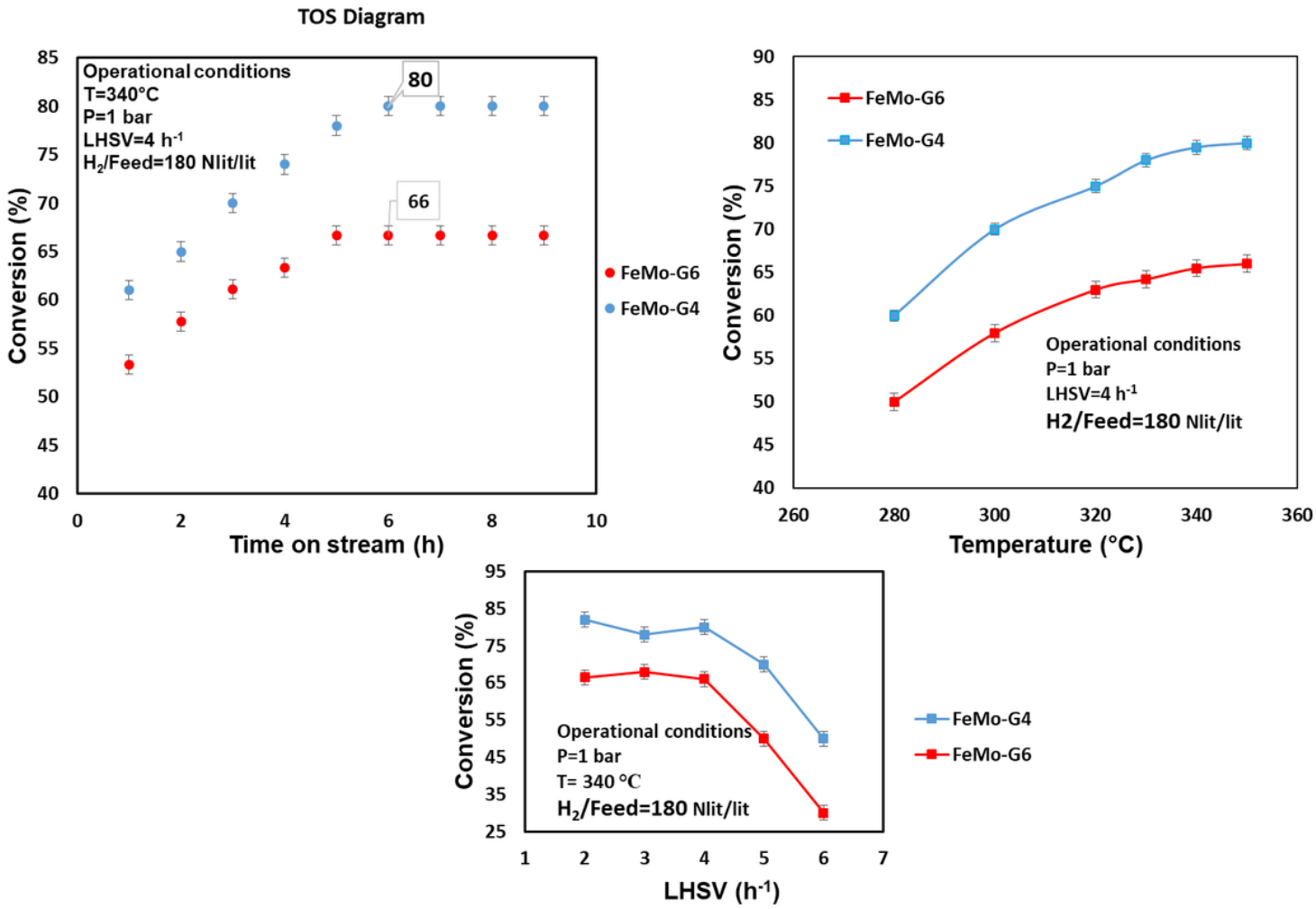

Figure 12

Comparison between FeMo-G4 and FeMo-G6 catalysts. Effect time, temperature and LHSV on conversion of catalysts.